ISSN 1063-7729, Astronomy Reports, 2019, Vol. 63, No. 11, pp. 891–899. © Pleiades Publishing, Ltd., 2019.
Russian Text © The Author(s), 2019, published in Astronomicheskii Zhurnal, 2019, Vol. 96, No. 11, pp. 898–906.

Correlation between the Distribution of Diffuse Ionized Gas in the Galaxy and HII Regions

A. V. Pynzar'*

Pushchino Radio Astronomy Observatory, Astro Space Center, P.N. Lebedev Physical Institute, Russian Academy of Sciences, Pushchino, Moscow region, 142290 Russia

Received April 19, 2019; revised May 31, 2019; accepted May 31, 2019

Abstract—The spatial correlation between HII region and diffuse ionized gas found earlier for the Hα line is confirmed using radio observations. In the inner part of the Galaxy, in the direction with coordinates $l = 30°$, $b = 0°$, the ionizing radiation from HII regions can propagate to distances $\leqslant$240 pc, although 75% of this ionizing radiation arrives at mean distances of only $\leqslant$7 pc. At the Galactic anti-center ($l = 186.^{\circ}6$, $b = 0.^{\circ}32$), the ionizing radiation of HII regions is able to ionize gas to distances of $\leqslant$1300 pc, although 66% of this radiation ionizes gas at distances of $\leqslant$155 pc. The relationship between the distributions of HII regions and diffuse ionized gas is used to derive the parameters of this gas in the direction of the pulsar B1758-23: emission measure 5800 ± 900 pc/cm^6, mean electron density in clouds 5.42 cm^{-3}, extent of the region occupied by clouds 200 pc, and filling factor for the electrons 0.06. The maximum contribution to the emission measure, dispersion measure, and scattering parameters of B1758-23 are made by a region at a distance of $\approx$1.3 kpc from the observer. The distance to PSR B1758-23 is found to be 3.5(+1, −0.3) kpc.

DOI: 10.1134/S1063772919110040

1. INTRODUCTION

About 20 years ago, a high degree of spatial correlation was found between the Hα emission from HII regions and diffuse ionized gas (DIG), both in other galaxies [1–6] and in our Galaxy [7]. It was hypothesized that, due to inhomogeneity in the distribution of gas in HII regions, some of the L_c photons (with wavelengths <912 Å) escape into interstellar space [6–9]. Due to the inhomogeneous distribution of neutral hydrogen and the presence in the medium of hot corridors and superenvelopes with temperatures $T \approx 10^6$ K and electron densities $N_e \approx 10^{-3}$ cm^{-3} [10], these photons can propagate far from the place they are produced, and are capable of ionizing gas at large distances from the sources of ionization [6–8].

It is of interest to search for similar correlations using radio data. We have investigated the connection between HII regions and DIG using the catalog of HII regions [11] and observations of the Galactic background in the H166α line [12]. The correlation found was used to determine the parameters of the DIG in the direction of the pulsar B1758-23.

2. REDUCTION METHOD

We selected objects from the catalog of HII regions [11] with measured velocities V, known distances D, and known excitation parameters U. We first determined the angular distances φ and impact parameters p for each HII region from the line of sight toward a given direction. For each HII region, we then determined the ratio

$$a = U/p^2.$$

The excitation parameter U is related to the number of L_c photons $N(L_c)$ radiated per second by the star forming the HII region as [10]:

$$N(L_c) \approx 3.8 \times 10^{43}[U/(\text{pc cm}^{-2})]^3 \text{ photons/s}, \quad (1)$$

where $U = r_s(N_e)^{2/3}$ pc/cm^2 and r_s and N_e are the radius of the Strömgren zone and the electron density in this zone.

The interstellar medium is very inhomogeneous. Dense clouds of neutral hydrogen (HI) and dust could be located in the line of sight toward an HII region. An HII region may be bright and close to the line of sight in a given direction, but dense clouds of dust or HI may absorb all the L_c photons emitted by the region. Therefore, the farther an HII region lies from a given line of sight, the higher the probability that its emission will be absorbed on its way to the observer. Assuming that the medium consisting of neutral hydrogen and dust is statistically uniform, it makes sense to give preference to HII regions that are closest to the line of sight.

To estimate the influence of HII regions observed at an angular distance φ from a given line of sight

*E-mail: pynz@prao.ru

on DIG in that direction, we calculated the sum of the parameters a for all HII regions at this angular distance from a given line of sight, $A = \sum a_i$. To calculate this parameter for a given direction, we chose only HII regions whose contributions to A were more than 1% of the contribution of the third greatest a value in this direction. The reason is that the highest value of a in a given direction can sometimes correspond to a weak HII region that is located very close to the line of sight. In this case, the value of $a = U/p^2$ is high due to the small impact parameter p, not because the HII region is bright. Rejected HII regions with very low a values can be used to estimate which of them at what distances from the observer make the maximum contribution to ionized gas in a given direction. The angular distance φ within which HII regions were considered depends on the direction in the Galaxy. The more HII regions there are in a given direction, and the brighter they are, the smaller the value of φ used. For example, $\varphi = 3°$ near Galactic longitude 30°, while $\varphi = 50°$ in the direction of the Galactic anti-center. The criteria used were such that the contribution of rejected HII regions to the total value $A = \sum a_i$ for all HII regions within the selected limiting angular distance not exceed 3%. When estimating the angular distance within which HII regions were considered, we first chose an obviously large angle. For example, in the directions of the inner Galaxy ($l = 4°$–$32°$, $b = 0°$), where the concentration of HII regions is high, we first chosen an angular distance of 10°. We calculated $A = \sum a_i$ within this angular distance, then decreased the limiting distance successively by 1°, calculating A each time. This was continued until the value of A reached ≈97% of the value of this parameter for an angular distance of 10°. For observations near the Galactic anti-center, the initial angular distance was taken to be 100° and the size considered was succesively decreased by 10°.

We will now present examples of our calculations of A for two directions in the Galaxy. In the direction with Galactic coordinates $l = 31°$ and $b = 0°$, 133 sources with known distances, velocities and excitation parameters were found with a radius of 4° from the line of sight in the catalog of HII regions [11]. The maximum value of a in this direction is 0.767 pc^{-1} cm^{-2}. The third greatest value is $a = 0.263$ pc^{-1} cm^{-2}. The summed value is $A = 2.423$ pc^{-1} cm^{-2}. After rejecting HII regions with $a < 0.001$ pc^{-1} cm^{-2}, 60 HII regions remained, with the summed value $A = 2.398$ pc^{-1} cm^{-2}. Thus, rejecting more than half the HII regions led to a reduction in A by only 1%.

In a direction close to the Galactic anti-center ($l = 186.^\circ6$ and $b = 0.^\circ32$), 99 HII regions were observed within 50° of the line of sight in the given direction. The maximum a value is $a = 0.00257$ pc^{-1} cm^{-2}, and the summed value is $A = 0.01587$ pc^{-1} cm^{-2}. The third greated value of a is 0.000834 pc^{-1} cm^{-2}. After rejecting HII regions with $a < 7 \times 10^{-6}$ pc^{-1} cm^{-2}, 63 HII regions remained, with $A = 0.01575$ pc^{-1} cm^{-2}. Rejecting 36 HII regions thus led to a reduction in A by only 0.76%.

3. RELATIONSHIP BETWEEN THE GALACTIC THERMAL BACKGROUND AND HII REGIONS

We searched for a relationship between HII regions and DIG by comparing the distributions of the HII regions and the background antenna temperature T_A in the H166α in a velocity—Galactic longitude diagram (Fig. 1). This comparison is justified, since T_A is proportional to the background emission measure [13]. Measurements of the background brightness in the H166α line were obtained for Galactic longitudes 4°–44.6° and Galactic latitude $b = 0°$ in [12] with a resolution of 21′. A similar survey of the Galactic plane in the H166α, H167α, and H168α recombination lines was carried out later [14–16], but in a narrower range of longitude ($l = 20°$–$44°$). Moreover, the brightness temperatures are presented only in the form of contours in [14–16], while the survey data of [12] are presented in tables, making the data more convenient for use in other studies. Accordingly, we used the data of [12] for our current study.

Data on HII regions were obtained near 5 and 8.6 GHz and collected in the catalog [11], as was noted above. The distribution of the background antenna temperature in the H166α line in a velocity—longitude diagram [12] for Galactic longitudes 30°–36° and $b = 0°$ is presented in Fig. 1. This figure is a fragment of Fig. 2 of [12]. Figures 2–4 of our paper present distributions of HII regions in velocity–distance diagrams for longitudes 31°, 33°, and 35°, respectively. As in [11] and [12], the velocities have been reduced to the Local Standard of Rest. The values of a in Figs. 2–4 are denoted using various symbols: line segments correspond to $a > 0.1$ pc^{-1} cm^{-2}, pluses to $a = 0.01$–0.1 pc^{-1} cm^{-2}, and filled circles to $a = 0.001$–0.01 pc^{-1} cm^{-2}. The numbers near the contours in Fig. 1 denote the corresponding background antenna temperature in the H166α line in Kelvin.

Comparison of Fig. 1 and Figs. 2–4 shows a large clustering of HII regions in Figs. 2–4 that corresponds to high antenna temperatures in Fig. 1. In contrast, the antenna temperatures are low in directions where there are no HII regions. It is sufficient to compare the data in these figures with the same

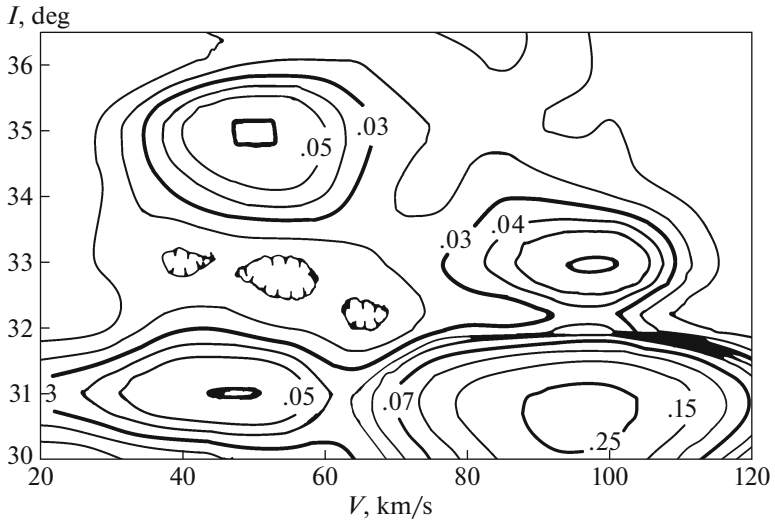

Fig. 1. Distribution of the background antenna temperature in a velocity–distance diagram for Galactic longitudes $l = 30°$–$36°$ and $b = 0°$. The numbers near the contours denote the background antenna temperature in the H166α line in Kelvin.

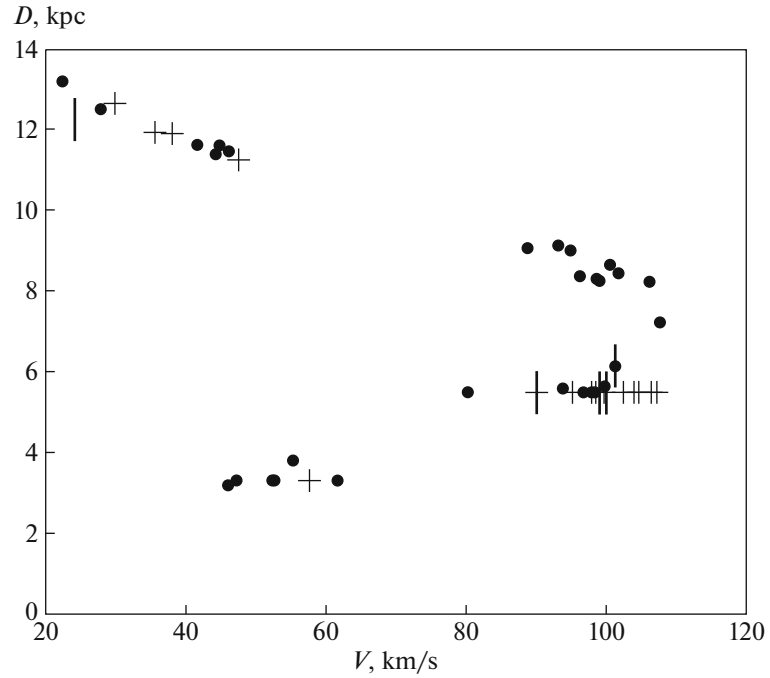

Fig. 2. Distribution of HII regions in a velocity–distance diagram for Galactic longitude $l = 31°$ and $b = 0°$. The values of $a = U/p^2$ are denoted by various symbols: vertical line segments correspond to $a > 0.1$ pc^{-1} cm^{-2}, pluses to $a = 0.01$–0.1 pc^{-1} cm^{-2}, and filled circles to $a = 0.001$–0.01 pc^{-1} cm^{-2}.

velocities and longitudes. For example, two maxima are observed in the H166α emission in Fig. 1 at longitude 31°: one that is weaker ($T_A = 0.07$ K) at velocities 30–60 km/s and another that is stronger ($T_A = 0.25$ K) at velocities 80–120 km/s, with a minimum in the emission ($T_A = 0.03$ K) observed at velocities 60–80 km/s. The ratio of the antenna temperatures of the stronger to the weaker maxima is ≈3.6.

Figure 2 shows that a large cluster of HII regions is observed in the direction of this longitude at velocities 80–110 km/s, which includes seven sources denoted by line segments and pluses. The sum of the a values for all HII regions within φ of the line

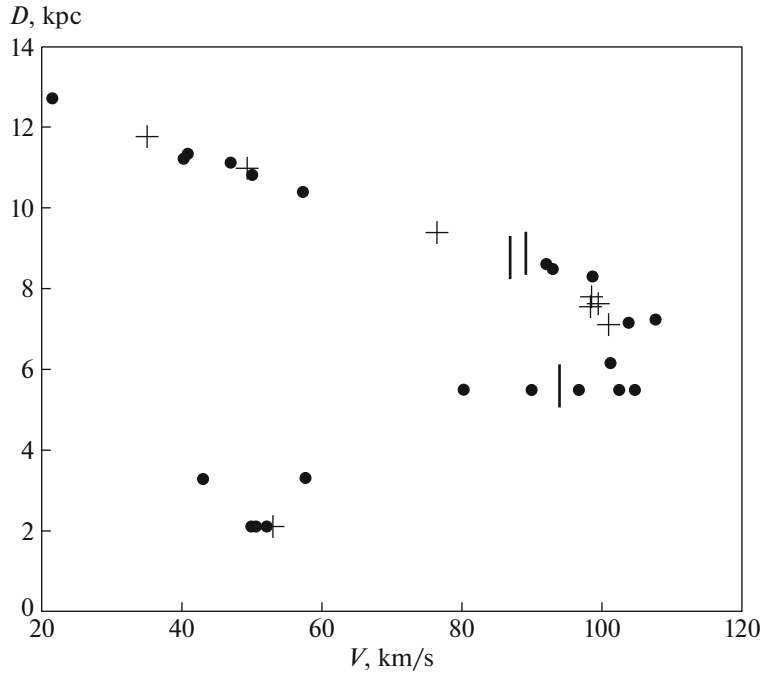

Fig. 3. Distribution of HII regions in a velocity—distance diagram for Galactic longitude $l = 33°$ and $b = 0°$. The notation is the same as in Fig. 2.

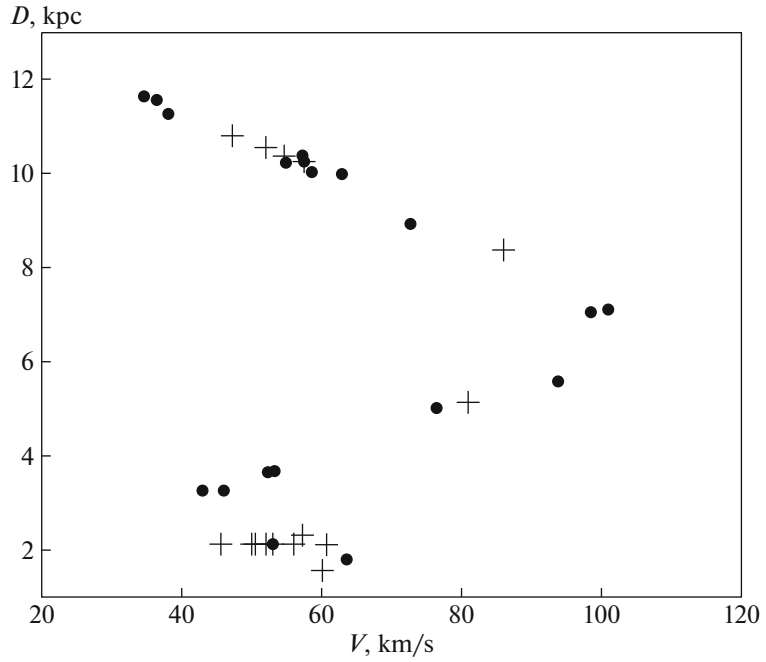

Fig. 4. Distribution of HII regions in a velocity–distance diagram for Galactic longitude $l = 35°$ and $b = 0°$. The notation is the same as in Fig. 2.

of sight in the given direction with velocities 80–110 km/s is $A = \sum a_i = 1.89$ pc^{-1} cm^{-2}, while $A = 0.53$ pc^{-1} cm^{-2} in the velocity interval 30–60 km/s, where there are fewer HII regions and those present are weaker. The ratio of the A values for the large cluster of HII regions and the smaller group is ≈3.6, consistent with the ratio of the antenna temperatures for the stronger and the weak maxima in Fig. 1. Only

two weak HII regions are observed at velocities 60–80 km/s, where there is a minimum in the H166α emission.

Thus, we can see from a comparison of Figs. 1 and 2 that there is a correlation between the distributions of HII regions and the antenna temperature in the H166α line. It follows that the distribution of HII regions can be used to estimate the distances to regions toward which maximum and minima in the DIG emission are observed in some directions. For example, as was noted above, a maximum in the H166α emission is observed at longitude 31° in the Galactic plane at velocities 80–120 km/s (Fig. 1). Figure 2 shows that two groups of HII regions are observed in this direction at the same velocities, the first located at distances of about 5.5 kpc with $A = 1.842$ pc^{-1} cm^{-2} and the second at distances of 7–9 kpc with $A = 0.046$ pc^{-1} cm^{-2}. It follows that the main contribution to the DIG emission is made by gas located at a distance of 5.5 kpc. In this same direction, two groups of HII regions are also observed at velocities 30–60 km/s: one at distances of 3–4 kpc, and the other at distances of 11–12 kpc (Fig. 2). The first group has $A = 0.049$ pc^{-1} cm^{-2}, and the second $A = 0.477$ pc^{-1} cm^{-2}. It follows that the main contribution to the DIG emission in the H166α line at velocities 30–60 km/s (Fig. 1) is made by HII regions at distances of 11–12 kpc. Thus, using observations of DIG emission and of HII regions, it is possible to determine not only the directions of maximum DIG emission, but also the distances at which the gas responsible for this emission is located.

The intensity of the H166α emission at 33° is strongest at velocities 80–110 km/s ($T_A = 0.07$ K, Fig. 1) and very weak at velocities 30–80 km/s ($T_A = 0.02$–0.03 K). Figure 3 shows that the number of HII regions and the a values are higher in this direction at 80–110 km/s than in the other velocity intervals. This is due to the fact that these sources are located close to the line of sight ($d = 6$–25 pc) in the given direction ($l = 33°$, $b = 0°$), while most of the HII regions located at velocities 40–60 km/s are located at distances of 70–250 pc from the line of sight. This means that an appreciable fraction of the ionizing radiation emerging from the HII regions is likely aborbed by neutral hydrogen and dust, and does not reach the line of sight.

The cluster of HII regions at velocities 35–65 km/s in the direction of longitude 35° is of interest. About half of these HII regions are located at distances of 9–12 kpc (Fig. 4), but they have small a values ($a = 0.001$–0.01 pc^{-1} cm^{-2}). The other half of the HII regions in the direction of this longitude are located at distances of about 2 kpc. The a values for these HII regions are an order of magnitude higher than the a values for the HII regions located at distances of 9–12 kpc.

Figure 1 shows that the antenna temperature at velocties 35–65 km/s is highest at longitude 35°, lower at 36°, and even lower at 36°.5. Although the values of a for the HII regions located at distances of 2 kpc (Fig. 4) are higher, on average, than those for the HII regions at distances of 9–12 kpc (as can be seen from the abundance of line segments and pluses for HII regions at distances of 2 kpc), they probably make only an insignificant contribution to the DIG emission in this direction. This is also indicated by the fact that the supernova remnants Kes 78 (G 32.8-0.1), Kes 79 (G 33.6+0.1), and W44 (G 34.7-0.4), located at distances of no less than 3 kpc, do not have turnovers in their spectra at 31 MHz due to absorption of their radiation by ionized gas [17]. It is possible that there is a large amount of dust in this direction, as is also suggested by the absence of optical HII regions [18, 19].

We present several dependences indicating the presence of a correlation between HII regions and DIG of the Galactic background. Figure 5 presents dependences on the parameter A of (a) the background antenna temperature in the H166α line, (b) the freqency-integrated values of T_A, P, and (c) the scattering angles for compact extragalactic sources θ at 1 GHz. The data for T_A and P were taken from [12]. The data on the scattering angles were taken from [20] (see also references therein) and [21] and reduced to 1 GHz proportional to the square of the wavelength. The dependences have been fitted with power-law functions of the form A^α. The power-law index $\alpha = 0.68 \pm 0.08$ in Fig. 5a, 0.75 ± 0.08 in Fig. 5b, and 1.0 ± 0.12 in Fig. 5c. All these quantities plotted as functions of A are proportional to the emission measure [13, 20, 22], that is, they characterize the background surface brightness. Figure 5 shows that these quanties are well correlated with A, indicating a relationship between the distributions of HII regions and of DIG.

4. DISTRIBUTION OF DIG IN THE DIRECTION OF THE PULSAR B1758-23

Figure 6 presents the distribution of HII regions toward the pulsar B1758-23 in a velocity–distance diagram. This figure shows that there are few HII regions toward this pulsar, and there are no objects with low values of a. As was noted above, the a values denoted by line segments exceed 0.1 pc^{-1} cm^{-2}. The fact that HII regions with such high a values are located toward B1758-23 suggests that the electron density in the DIG is fairly high, as we will show below. Figure 6 also shows that the HII regions with

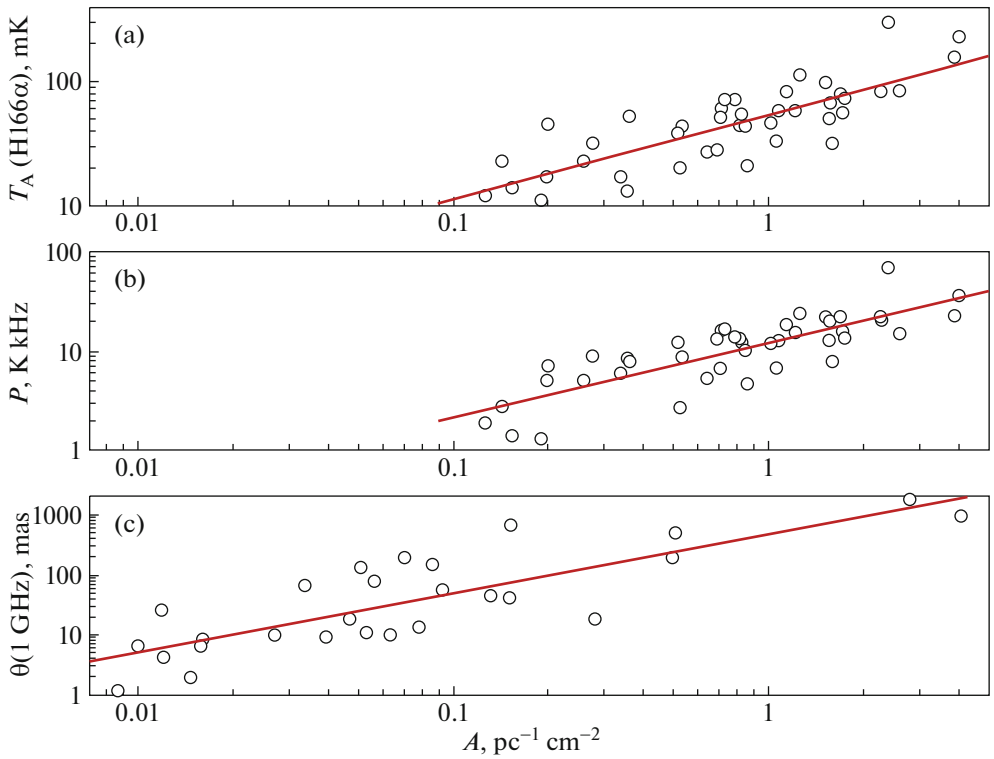

Fig. 5. (a) Background antenna temperatures T_A in the H166α line, (b) freqency-integrated values of T_A, P, and (c) the scattering angles for compact extragalactic sources θ at 1 GHz as functions of the parameter A. The data for T_A and P were taken from [12]. The data on the scattering angles were taken from [20] and [21] and reduced to 1 GHz proportional to the square of the wavelength. The dependences have been fitted with power-law functions of the form A^α. The power-law index $\alpha = 0.68 \pm 0.08$ in panel (a), 0.75 ± 0.08 in panel (b), and 1.0 ± 0.12 in panel (c).

the highest a values are located in a narrow range of distances. The five HII regions denoted by line segments and two more denoted by pluses are located at distances 1.28 ± 0.09 kpc [11]. These HII regions contribute 80% of A, which is the sum of the a values for all HII regions within 3° of the line of sight toward the pulsar. The summed parameter A in this direction is 3.81 pc^{-1} cm^{-2}, which is the highest value of this parameter in the first quadrant of the Galaxy.

As was shown above, the highest a values are possessed by HII regions located at a distance of 1.28 kpc. This indicates that, with high probability, precisely these HII regions are responsible for ionizing the neutral hydrogen in this direction. Using the a values for these HII regions and their distances from the line of sight toward B1758-23, we found that 97% of the ionizing radiation from HII regions toward this pulsar arrives from distances $\leqslant$18 pc from the pulsar's line of sight, and 87% arrives from distances $\leqslant$9 pc.

Since HII regions located 1.28 kpc from the observer contribute 80% of the total A value, this suggests that the associated DIG is concentrated in a thin layer; in other words, the thickness of the layer in which the HII regions are concentrated is much smaller than the distance to the layer (Fig. 6). A small thickness for the effective layer of ionizing gas is also indicated by the fact that 87% of the ionizing radiation from HII regions arrives from distances $\leqslant$9 pc.

To demonstrate that the effective layer of DIG toward B1758-23 is located at a distance of about 1.3 kpc, we determined the distance to the pulsar based on broadening of the pulses due to interstellar scattering τ, then compared this with the distance estimated in [23] based on measurements of aborption of the pulsar emission in the 21-cm neutral-hydrogen line.

To establish a relationship between the broadening of the pulsar pulses τ, the distance to the pulsar, and the distance to the layer making the main contribution to the interstellar scattering, it is convenient to use the following formula for a model scattering medium in the form of a thin screen [24, 25]:

$$\tau = [\theta^2/(8c\ln 2)][d(D-d)/D], \qquad (2)$$

where D is the distance from the observer to the pulsar, d the distancee from the observer to the scattering screen, and θ the scattering angle (width of the scattering disk at the 0.5 level) of a compact source of plane waves, such as an extragalactic source, whose radiation passes through the same medium

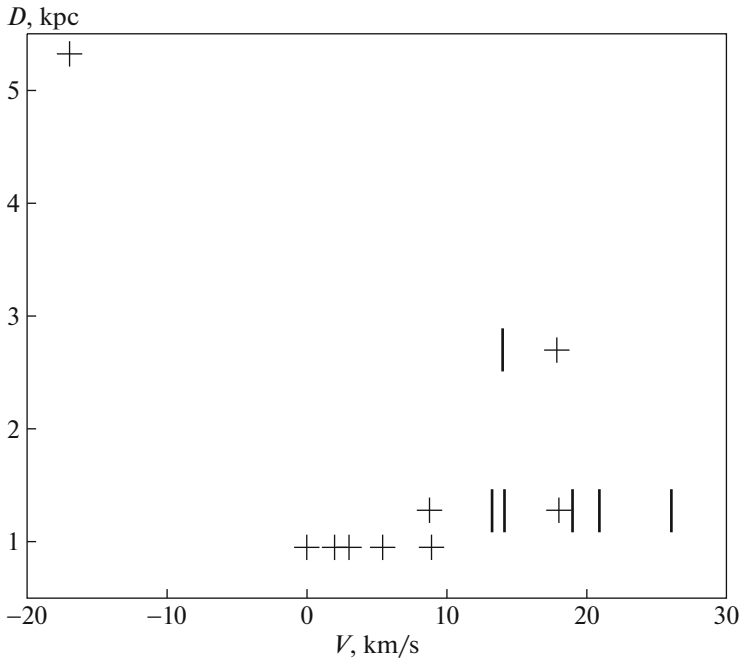

Fig. 6. Distribution of HII regions toward the pulsar B1758-23 in a velocity–distance diagram. Notation is the same as in Fig. 2.

as a source of spherical waves (the pulsar in our case). Formula (2) indicates that the broadening of the pulsar pulses depends on the factor $d(D-d)/D$. This factor is close to zero for layers close to the pulsar ($D-d\approx 0$) or close to the observer $d\approx 0$, and reaches a maximum when the scattering medium is located roughly halfway between the observer and pulsar ($d=D/2$). We emphasize that this formula relates the broadening of the pulses in time with the scattering angle of an extragalactic (plane-wave) source whose radiation passes through the same layer of scattering medium. We chose the extragalactic source J1801-231 located at an angular separaton of 1′.6 from the pulsar for the source of plane waves, and assumed that the parameters of the DIG in the directions of both sources are the same. This is justified by the fact that the effective scattering layer is located between the observer and pulsar, and the ionized medium at distances exceeding the distance to the layer, $d\approx 1.3$ kpc, does not significantly influence the scattering of the extragalactic source, as can be seen from the absence of HII regions with large a values at distances exceeding 1.3 kpc (Fig. 6).

The pulse broadening values for B1758-23 were taken from [26], and the scattering-angle values for J1801-231 from [27]. Measurements of these parameters made at various frequencies are provided in these studies. We used the frequency dependences of these parameters to determine their values at 1 GHz: $\tau=0.32\pm0.02$ s, $\theta=0.95\pm0.06$ arcsec.

To determine the distance to B1758-23, we rewrote (2) in the form

$$D=(0.436\theta^2d^2)/(0.436\theta^2d-\tau)\ \text{kpc}. \qquad (3)$$

Using the above values of τ and θ and the distance to the effective DIG layer $d=1.28\pm0.09$ kpc [11], we estimated the distance to B1758-23 using (3) to be 3.5 kpc. Taking into account the uncertainties in τ, θ, and d, the inferred distance D lies in the range ≈3.2–4.5 kpc. This is in agreement with the value $D=4\pm1$ kpc obtained in [23] based on measurements of the absorption of the pulsar radiation in the 21-cm line of neutral hydrogen. The agreement between the distances to the pulsar B1758-23 obtained using these two independent methods testifies that the method we have described here is reliable. The estimate of the distance to the effective layer of ionized medium that we derived by comparing the distributions of HII regions and DIG is likewise trustworthy. This all indicates the existence of a high degree of correlation between the distributions of HII regions and DIG in the Galaxy.

Let us estimate some parameters of the DIG responsible for the dispersion measure and pulse broadening of B1758-23. It is known that DIG in the Galaxy has a cloud-like structure [28–31]. The emission measure EM and dispersion measure DM can be used to estimate the local (mean in clouds) electron density N_e, the total path in the clouds along the line of sight L_e, and the filling factor F_e. L_e is the effective thickness of the medium filled by clouds of ionized

gas, and F_e indicates what fraction of the volume of the medium along the line of sight toward the pulsar is occupied by this gas. These quantities were calulated using the formulas [32]:

$$N_e = EM/DM, \quad (4)$$

$$L_e = DM^2/EM, \quad (5)$$

$$F_e = \langle N_e \rangle / N_e, \quad (6)$$

where $\langle N_e \rangle = DM/D$ is the mean electron density along the line of sight toward the pulsar, located a distance D from the observer.

The background emission measure toward B1758-23 is 5800 ± 900 pc/cm^6. The emission measure was estimated using the method and data presented in [20]. The dispersion measure of the pulsar, 1073.9 pc/cm^3, was taken from the pulsar catalog [33]. We obtained $N_e = 5.42$ cm^{-3}, $L_e =$ 200 pc, $\langle N_e \rangle = 0.31$ cm^{-3}, and $F_e = 0.057$ in the direction toward B1758-23.

5. DISCUSSION

The question of how far radiation from sources of ionization propagates in the interstellar medium has been widely discussed in the literature ([8] and references therein). We tried to estimate these distances for the directions with Galactic coordinates $l = 30°$, $b = 0°$ and $l = 186.^\circ6$, $b = 0.^\circ32$ using the values of a for the HII regions and the corresponding distances to the line of sight in these directions. We found that, in the inner part of the Galaxy ($l = 30°$, $b = 0°$), >1% of the ionizing radiation within 3° of the indicated direction arrives from mean distances $\leqslant$240 pc, with 75% of the radiation arriving from mean distances $\leqslant$7 pc. At the Galactic anti-center ($l = 186.^\circ6$, $b = 0.^\circ32$), >1% of the ionizing radiation within 50° arrives from mean distances $\leqslant$1300 pc, with 93% arriving from distances $\leqslant$245 pc, and 66% from distances $\leqslant$155 pc.

The presence of a correlation between the distributions of HII regions and DIG in the Galaxy opens possibilities for refining models of the distribution of the electron concentration in the Galaxy [34]. Knowing the DIG distribution, it is possible in some cases to determine distances to pulsars and supernova remnants with spectral turnovers at low frequencies when this is not possible using more traditional methods.

Knowledge of the DIG distribution also makes it possible to explain why pulsars in some directions in the Galaxy with moderate dispersion measures display fairly high pulse broadening and, on the contrary, some pulsars with high dispersion measures may display low broadening.

6. CONCLUSION

1. We have confirmed the correlation between HII regions and diffuse ionized gas detected earlier in the optical using radio observations.

2. Based on the correlation between HII regions and DIG, we have proposed a method that can be used to investigate the parameters of the DIG.

3. We have determined the parameters of the DIG toward the pulsar B1758-23 and determined the pulsar's distance to be 3.5(+1, −0.3) kpc.

4. We have shown that the distances to which ionizing radiation from sources of such radiation can propogate depend on the gas density. In the inner part of the Galaxy (for example, in the direction $l = 30°$, $b = 0°$), L_c photons can ionize gas within 3° of the light of sight to mean distances $\leqslant$240 pc, with 75% of this radiation ionizing gas to mean distances $\leqslant$7 pc. In the direction of the Galactic anti-center (e.g., $l = 186.^\circ6$, $b = 0.^\circ32$), the ionizing radiation within 50° of the line of sight reaches mean distances $\leqslant$1300 pc, with 93% reaching distances $\leqslant$245 pc, and 66% distances $\leqslant$155 pc.

ACKNOWLEDGMENTS

The author thanks R.D. Dagkesamanskii and the referee for valuable comments, and T.V. Smirnova and V.A. Izvekova for useful discussions.

REFERENCES

1. R. A. M. Walterbos and R. Braun, Astrophys. J. **431**, 156 (1994).
2. A. M. Ferguson, R. F. G. Wyse, J. S. Galagher, and D. A. Hunter, Astron. J. **111**, 2265 (1996).
3. S. G. Hoopes, R. A. M. Walterbos, and B. E. Greenawalt, Astron. J. **112**, 1429 (1996).
4. S. G. Hoopes, R. A. M. Walterbos, and R. J. Rand, Astrophys. J. **522**, 669 (1999).
5. A. E. Zurita, M. Rozas, and J. E. Beckman, Astron. Astrophys. **363**, 9 (2000).
6. A. E. Zurita, J. E. Beckman, M. Rozas, and S. Ryder, Astron. Astrophys. **386**, 801 (2002).
7. R. J. Reynolds, N. C. Sterling, and L. M. Haffner, Astrophys. J. **558**, L101 (2001).
8. L. M. Haffner, R.-J. Dettmar, J. E. Becman, K. Wood, et al., Rev. Mod. Phys. **81**, 969 (2009).
9. N. A. Kassim, K. W. Weiler, W. C. Erickson, and T. L. Wilson, Astrophys. J. **338**, 152 (1989).
10. S. A. Kaplan and S. B. Pikel'ner, *Physics of the Interstellar Medium* (Nauka, Moscow, 1979) [in Russian].
11. L. G. Hou and J. L. Han, Astron. Astrophys. **569**, 125 (2014).
12. F. J. Lockman, Astrophys. J. **209**, 429 (1976).
13. F. J. Lockman, D. J. Pisano, and G. J. Howard, Astrophys. J. **472**, 173 (1996).

14. M. I. R. Alves, R. D. Davies, C. Dickinson, R. J. Davis, R. R. Auld, M. Calabretta, and L. Staveley-Smith, Mon. Not. R. Astron. Soc. **405**, 1654 (2010).
15. M. I. R. Alves, R. D. Davies, C. Dickinson, M. Calabretta, R. Davis, and L. Staveley-Smith, Mon. Not. R. Astron. Soc. **422**, 2429 (2012).
16. M. I. R. Alves, M. Calabretta, R. D. Davies, C. Dickinson, et al., Mon. Not. R. Astron. Soc. **450**, 2025 (2015).
17. N. E. Kassim, Astrophys. J. **347**, 915 (1989).
18. S. Sharpless, Astrophys. J. Suppl. Ser. **4**, 257 (1959).
19. B. T. Lynds, Astrophys. J. Suppl. Ser. **12**, 163 (1965).
20. A. V. Pynzar', Astron. Rep. **54**, 386 (2010).
21. A. B. Pushkarev and Y. Y. Kovalev, Mon. Not. R. Astron. Soc. **452**, 4274 (2015).
22. A. L. Fey, S. R. Spangler, and J. M. Cordes, Astrophys. J. **372**, 132 (1991).
23. J. P. W. Verbiest, J. M. Weisberg, A. A. Chael, K. J. Lee, and D. R. Lorimer, Astrophys. J. **755**, 39 (2012).
24. K. M. Desai, C. R. Gwinn, J. Reynolds, E. A. King, et al., Astrophys. J. **393**, L75 (1992).
25. A. V. Pynzar', Astron. Rep. **61**, 417 (2017).
26. W. Lewandowski, M. Kowalinska, and J. Kijak, Mon. Not. R. Astron. Soc. **449**, 1570 (2015).
27. M. J. Claussen, W. M. Goss, K. M. Desai, and C. J. Brogan, Astrophys. J. **580**, 909 (2002).
28. J. M. Cordes, J. M. Weisberg, and V. Boriakoff, Astrophys. J. **288**, 221 (1985).
29. A. V. Pynzar', Astron. Rep. **37**, 245 (1993).
30. A. V. Pynzar' and V. I. Shishov, Astron. Rep. **41**, 586 (1997).
31. A. V. Pynzar' and V. I. Shishov, Astron. Rep. **43**, 436 (1999).
32. R. J. Reynolds, Astrophys. J. **216**, 433 (1977).
33. R. N. Manchester, G. J. Hobbs, A. Teoh, and M. Hobbs, Astron. J. **129**, 1993 (2005).
34. J. M. Yao, R. N. Manchester, and N. Wang, Astrophys. J. **835**, 29 (2017).

Translated by D. Gabuzda